1998

Spatial Contact Analysis of Fixed- Axes Pairs Using Configuration Spaces

Iddo Drori

Leo Joskowicz

Elisha P. Sacks
Purdue University, eps@cs.purdue.edu

Report Number:
98-032

SPATIAL CONTACT ANALYSIS OF FIXED-AXES PAIRS USING CONFIGURATION SPACES

Iddo Drori
Leo Joskowicz
Elisha Sacks

CSD-TR #98-032
September 1998

Spatial Contact Analysis of Fixed-Axes Pairs Using Configuration Spaces

Iddo Drori and Leo Joskowicz
Institute of Computer Science
The Hebrew University
Jerusalem 91904, ISRAEL

Elisha Sacks
Computer Science Department
Purdue University
West Lafayette, IN 47907, USA

Abstract

We present the first configuration space computation algorithm for pairs of rigid parts that move along fixed spatial axes. The motivation is contact analysis for mechanical design of spatial systems and of planar systems with axis misalignment. The part geometry is specified in a parametric boundary representation using planes, cylinders, and spheres. Our strategy is to exploit the specialized part geometry and the two-dimensional structure of the configuration space to obtain a practical algorithm. The main technical contribution is our derivation of low-degree algebraic contact equations in the two part motion parameters, which can readily be solved to obtain contact curves. We demonstrate a preliminary implementation on three representative pairs, none of which is covered by prior contact analysis algorithms. We show how the program is used to answer design questions.

1 Introduction

We present a contact analysis algorithm for pairs of rigid parts that move along fixed spatial axes. The motivation for this algorithm is computer-aided design of mechanical systems. Systems perform functions by transforming motions via part contacts. The shapes of the interacting parts impose constraints on their motions that largely determine the system function. Contact analysis is the task of deriving this evolving sequence of contacts and motion constraints. Designers use the results to simulate system function, to find and correct design flaws, to measure performance, and to compare design alternatives.

Prior research provides contact analysis algorithms for specialized systems. Mechanical simulation research [1, 2] focuses on efficient methods of solving the contact constraints of permanent contact assemblies, such as linkages and manipulators. Research in gear design [3] and in cam design [4] addresses individual contacts and specialized geometry, such as helical gears, worm gears, and spatial cams. Graphics research [5, 6, 7] provides fast collision detection algorithms for polyhedra, which support the contact analysis needs of simulation, but do not address the other aspects of contact analysis in mechanical design, such as tolerancing. Robot motion planning research [8] provides contact analysis algorithms for a polyhedral robot moving amidst fixed polyhedral obstacles. Many of the algorithms are based on configuration space computation.

This prior research does not provide practical contact analysis algorithms for pairs of curved parts with contact changes. Such pairs are very common in mechanical design. The most important class is planar pairs. We developed the first comprehensive contact analysis algorithm for planar pairs based on configuration space computation [9, 10]. We developed novel mechanical system simulation and tolerancing techniques and demonstrated them on a variety of planar mechanisms [11, 12].

In this paper, we extend the configuration space computation algorithm to pairs of parts that rotate around or translate along fixed spatial axes. This is the second most important class for mechanical design. Most spatial pairs move along fixed-axes according to a survey of 2500 mechanisms from an encyclopedia [13] and based on our experience. Spatial fixed-axes parts are a good way to model planar parts whose motion axes are misaligned due to wear, assembly error, or manufacturing variation. Thus, our analysis supports spatial tolerancing of nominally planar systems. The part geometry is specified in a parametric boundary representation using planes, cylinders, and spheres. This class covers almost all planar parts and most spatial parts, except for spatial gears and cams.

Our strategy is to exploit the specialized part geometry and the two-dimensional structure of the configuration space to obtain a practical algorithm. The main technical contribution is a derivation of low-degree algebraic contact equations in the two part degrees of freedom that can readily be solved to obtain contact curves. Prior derivations, such as Baraff [5], provide high-degree systems of equations that are impractical to solve. We combine the curves into a configuration space with our fixed-axes algorithm [9]. We demonstrate a preliminary implementation on three representative pairs, none of which is covered by

prior contact analysis algorithms. We show how the program is used to answer design questions.

2 Contact analysis

This section presents three representative spatial pairs that illustrate spatial contact analysis using configuration spaces. The configuration space of a pair is a complete representation of the part interactions: any contact question is answerable by a configuration space query. It encodes quantitative information, such as part motion paths, and qualitative information, such as contact changes and failure modes.

The configuration space is a two-dimensional manifold whose coordinates are the part degrees of freedom. It is a torus when both parts rotate, a cylinder when one rotates, and a plane when both translate. It partitions into blocked space where the parts overlap, free space where they do not touch, and contact space where they touch without overlap. The contact space partitions into contact curves that represent contact between pairs of part features.

The first example is a planar cam/follower pair (Figure 1(a)). The cam has a constant-breadth profile consisting of three arc segments. The follower has a rectangular profile. Nominally, the cam rotates around an orthogonal axis and the follower translates vertically. Each cam rotation makes the follower go up and down three times. The narrow gap between the parts prevents jamming.

Figure 1(b) shows the configuration space. The gray area is blocked space, the black curves are contact space, and the white area in between is free space. Contact space consists of upper and lower sinusoids that correspond to the contact between the cam and the lower and upper follower horizontals. Each consists of three pairs of alternating vertex/line and arc/line contact curves. The gap between the sinusoids quantifies the play, which varies with the cam orientation. The design question is whether axis misalignment causes jamming and if so whether widening the gap ensures correct function.

To answer these questions, we need to perform a spatial contact analysis on the planar pair. The axis misalignment transforms the contacts between planar features into spatial ones. For example, the arc/line contact becomes a cylinder/plane contact. Figure 1(c) shows the configuration space with the cam axis tilted by 0.75 degrees. The gap between the parts shrinks, which causes the play to shrink. Tilting the axis by 1 degree breaks the free space into six disconnected pieces, which indicates that the cam cannot complete a full cycle (jamming).

The second example is a pair of orthogonal spatial gears (Figure 2(a)). The gears are cylindrical plates with five

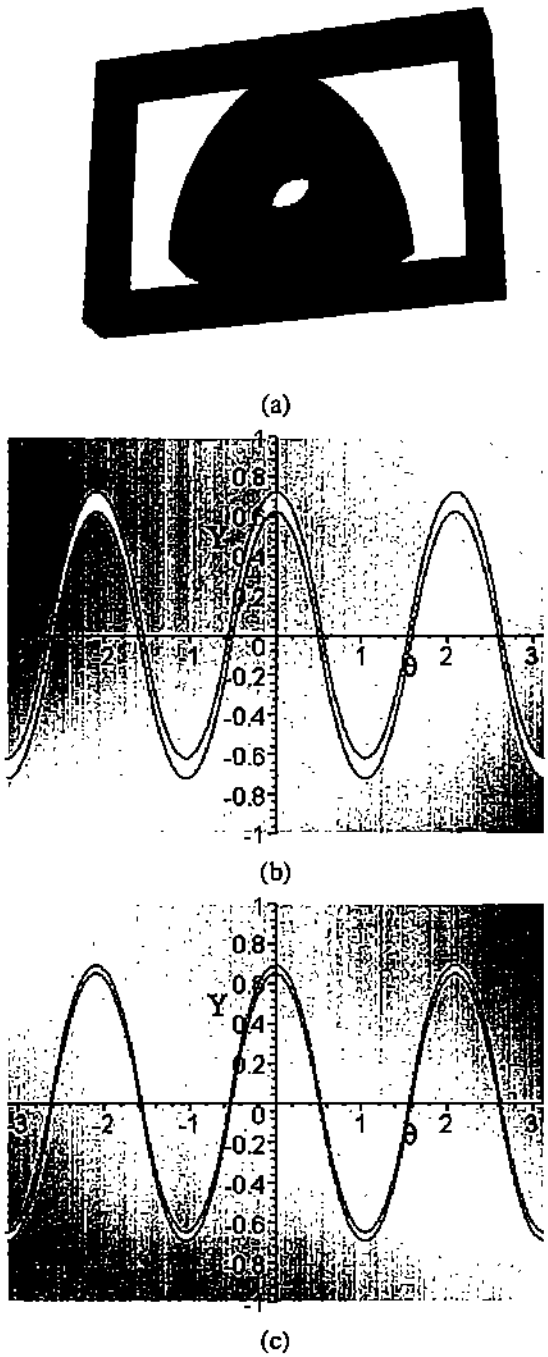

Figure 1: (a) Constant-breadth cam/follower, (b) its configuration space, (c) configuration space with tilted cam axis. Parameters θ and Y are the orientation of the cam and the vertical displacement of the follower.

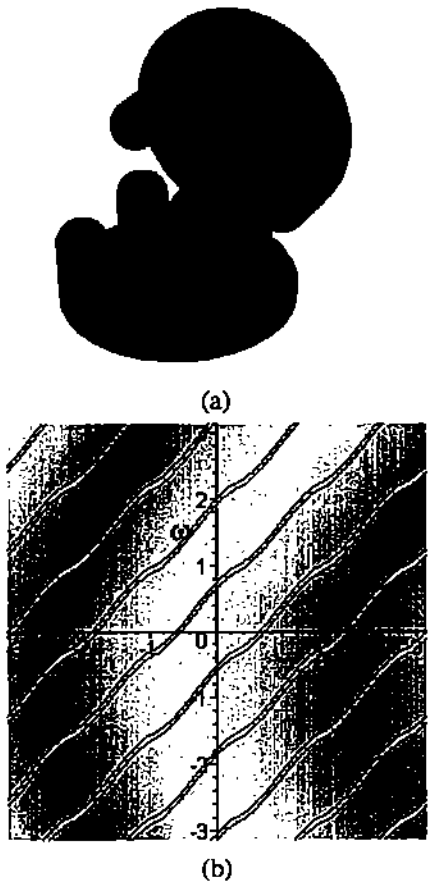

Figure 2: (a) Orthogonal gears and (b) their configuration space. Parameters θ and ω are the horizontal and vertical gear orientations.

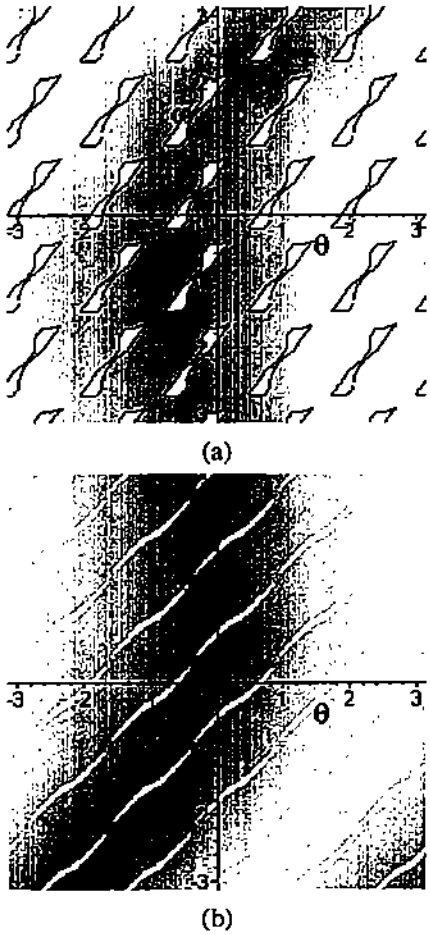

Figure 3: Configuration space of orthogonal gear pair with (a) longer teeth and (b) tilted axis.

evenly spaced teeth, which are cylinders topped by truncated spheres. The gears rotate around their axes. Rotating one causes the other to rotate by the same angle. Unlike the first example, the nominal system exhibits spatial contacts. Figure 2(b)) shows its configuration space. The contact space represents contacts between tooth sides, caps, and tops (cylinders, spheres, and planes). It shows a nearly linear gear ratio. The free space consists of five narrow channels that quantify gear play.

The design goal is to optimize the gear placement, tooth shape, and tooth spacing for smooth drive with minimal play. We need to analyze the contacts between pairs of teeth and the contact changes due to teeth meshing and unmeshing. Figure 3 shows configuration spaces with teeth length 6.2 cm instead of 5 cm and with one axis tilted by 0.8 degrees. The free space is broken into 25 disconnected regions which indicates that the gears jam. The teeth cannot unmesh because they are either too high or misaligned. Each free space region shows how much the gears can

move when a specific pair of teeth engages. With longer teeth, the contact relation between tooth sides is as before, but the contact curves are longer, intersect, and thus disconnect the free space. With a slanted axis, all the contacts are affected, so the free space is disconnected and changes shape.

The third example is a spatial Geneva pair (Figure 4). The cam is a plate with a pin and a half cylinder mounted on it. The follower is a hollow hemisphere with four evenly spaced slots and circular cutouts. The cam rotates around an axis through the cylinder center and the follower rotates around a vertical axis. As the cam rotates, the pin engages a follower slot and rotates by 90 degrees. When the pin disengages, the cam cylinder engages a follower cutout and prevents it from moving until the pin engages the next slot. The contact space contains four diagonal regions where the pin drives the follower, and four vertical regions where cylinder engages the cutouts. The design task is to find a pin angle and a slot clearance that guarantee the correct contact sequence. For example, if the pin reaches the slot too soon it hits the side and blocks.

3 Configuration space computation

We compute configuration spaces by the method that we developed for planar pairs with two-dimensional configuration spaces [9]. We enumerate the pairs of part features and generate contact curves for each pair. The curves partition configuration space into connected components. We compute the components with a customized line sweep algorithm and retrieve the components that bound free space regions. The algorithm handles the many degenerate cases that arise in practice. The only change for spatial pairs is contact curve computation.

Contact between two parts occurs when their boundaries intersect, but not their interiors. The contact points satisfy geometric constraints that depend on the dimension and geometry of the touching features. For example, when two faces touch, the outward normals at the contact point are collinear with opposite directions. The constraints for face/edge, face/vertex, edge/edge, and edge/vertex contacts are analogous. In each case, the constraint is expressible as an algebraic equation in the part angles. The set of real solutions consists of configuration space curves.

The contact equations apply to algebraic features: planes, cylinders, spheres, lines, circles, and points. Two part features touch when they contain the contact point of their algebraic features. For example, a line segment touches a hemisphere when the line is tangent to the sphere and the contact point lies on the segment and on the hemisphere. This means that the feature parameters of the contact point are in the allowable range. For the features that

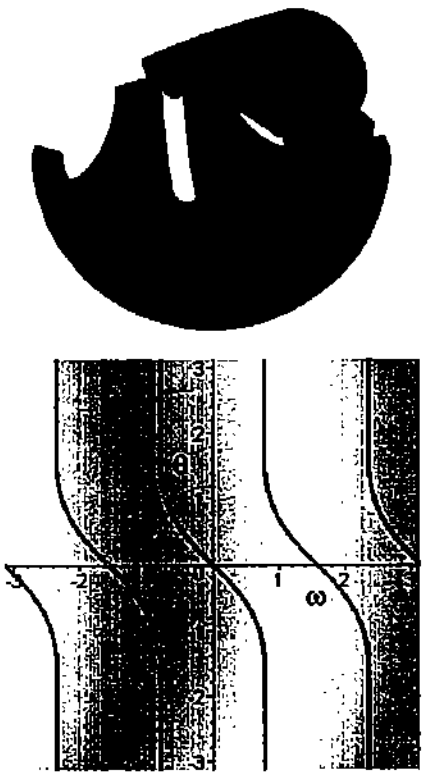

Figure 4: Spatial Geneva pair and its configuration space. Parameters θ and ω are the cam and follower orientations.

we study, it is easy to compute the parameters of the contact point, which allows us to test the contact conditions.

We can solve the contact equations in closed-form or numerically. A closed-form solution is faster and more robust, but may not be available. Our choice of part geometry allows us to formulate equations that have closed-form solutions in most cases and that are otherwise readily solved by standard numerical methods. Given the solution curve, we need to extract the contact curve, which is the subset where the feature parameters are in range. We compute the configurations where the parameters equal their endpoint values by the bisection method. An exact solution based on Sturm sequences is also possible. These values partition the curves into in-range and out-of-range intervals. The former are the contact curves.

4 Contact equations

We derive the contact equations and contact points for all pairs of features. We analyze cylinder/cylinder, cylinder/sphere, plane/sphere, cylinder/circle, plane/circle and sphere/circle. The other pairs are subsumed by these cases:

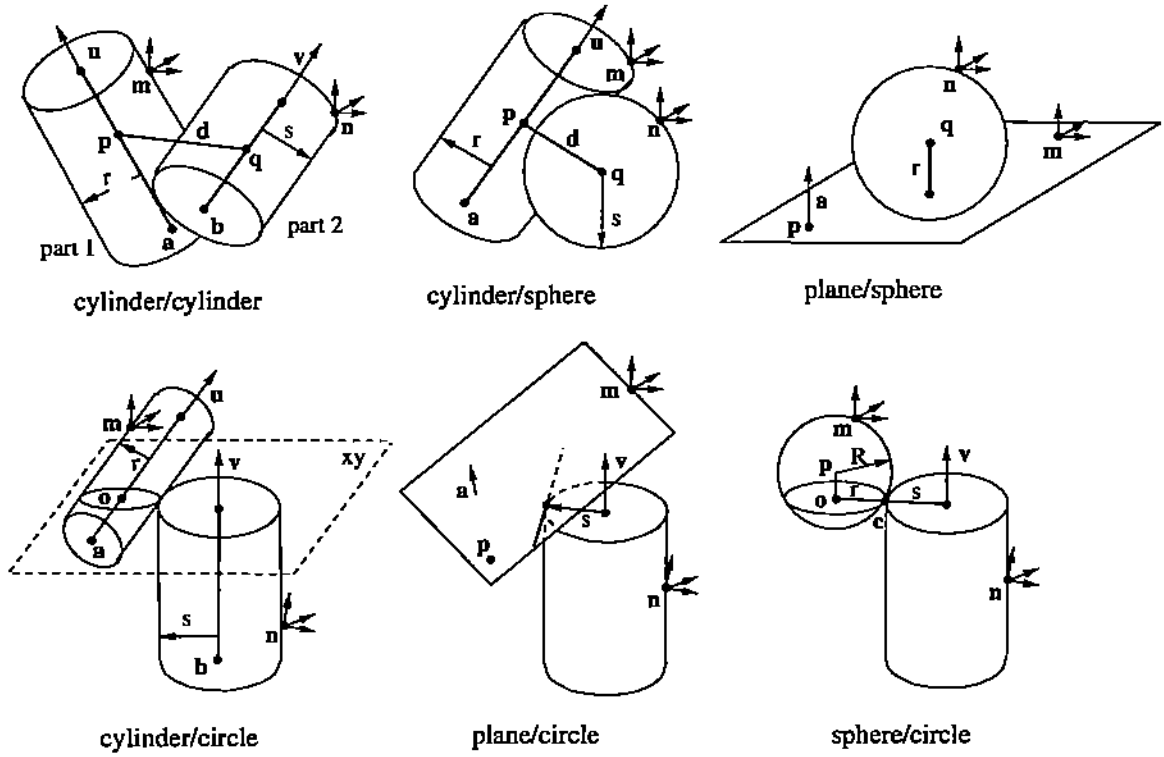

Figure 5: Six types of contacts.

vertices and lines are equivalent to spheres and cylinders of radius zero. Plane/plane and plane/cylinder contacts occur at finite sets of configurations, hence do not form contact curves. Circle/circle contacts are special cases of cylinder/circle. We assume that the rotation axes are skew; parallel axes are covered in prior work [9].

Figure 5 illustrates the six types of contacts. A point $\mathbf{p}_0$ in part 1 coordinates has global coordinates $\mathbf{p} = \mathbf{m} + R_\theta \mathbf{p}_0$ with $\mathbf{m}$ the part reference point, θ the rotation angle around the part rotation axis, and R_θ the rotation matrix. A point $\mathbf{q}_0$ in part 2 coordinates has global coordinates $\mathbf{q} = \mathbf{n} + R_\psi \mathbf{q}_0$. We use this notation throughout the section.

4.1 cylinder/cylinder

Contact occurs when the distance between the cylinder axes equals the sum of their signed radii. The sign is positive when the outward normal points out of the cylinder, negative when it points into the cylinder, and zero when the cylinder is a line. The sum of the radii must be positive for contact to occur. The distance equals the length of the line segment $\mathbf{d} = \mathbf{p} - \mathbf{q}$ that connects the cylinder axes and is orthogonal to both axes. We have $\mathbf{p} = \mathbf{m} + R_\theta(\mathbf{a}_0 + \alpha \mathbf{u}_0)$ with $\mathbf{u}_0$ a unit vector along the cylinder axis, $\mathbf{a}_0$ the point on the axis closest to the part origin, and α a scalar parameter. We have $\mathbf{q} = \mathbf{n} + R_\psi(\mathbf{b}_0 + \beta \mathbf{v}_0)$. Define $\mathbf{a} = R_\theta \mathbf{a}_0$, $\mathbf{u} = R_\theta \mathbf{u}_0$, $\mathbf{b} = R_\psi \mathbf{b}_0$, and $\mathbf{v} = R_\psi \mathbf{v}_0$. The orthogonality conditions are $\mathbf{d} \cdot \mathbf{u} = \mathbf{d} \cdot \mathbf{v} = 0$. This is a system of two linear equations for α, β whose solution is

$$\alpha = \frac{(\mathbf{b} + \mathbf{n} - \mathbf{m}) \cdot \mathbf{u} + (\mathbf{u} \cdot \mathbf{v})(\mathbf{a} \cdot \mathbf{v})}{1 - (\mathbf{u} \cdot \mathbf{v})^2} \quad (1)$$

$$\beta = \frac{(\mathbf{a} + \mathbf{n} - \mathbf{m}) \cdot \mathbf{v} + (\mathbf{u} \cdot \mathbf{v})(\mathbf{b} \cdot \mathbf{u})}{1 - (\mathbf{u} \cdot \mathbf{v})^2} \quad (2)$$

The solution uses the identities $\mathbf{a} \cdot \mathbf{u} = \mathbf{b} \cdot \mathbf{v} = 0$, which follow from the choices of $\mathbf{a}_0$ and $\mathbf{b}_0$ as closest points to the part origins, and $\mathbf{u}^2 = \mathbf{u}_0^2 = 1$, $\mathbf{v}^2 = \mathbf{v}_0^2 = 1$ which follow from the invariance of length under rotation. The contact equation is $\mathbf{d}^2 = (r + s)^2$ with r and s the signed radii. We simplify this equation to

$$\alpha(\mathbf{b} \cdot \mathbf{u}) + \beta(\mathbf{a} \cdot \mathbf{v}) + 2\mathbf{a} \cdot \mathbf{b} + (\mathbf{m} - \mathbf{n}) \cdot (\mathbf{a} + \alpha \mathbf{u} - \mathbf{b} - \beta \mathbf{v}) = k$$

with $k = \mathbf{a}_0^2 + \mathbf{b}_0^2 - (r + s)^2 - (\mathbf{m} - \mathbf{n})^2$ a constant with $\mathbf{a} \cdot \mathbf{u} = \mathbf{b} \cdot \mathbf{v} = \mathbf{d} \cdot \mathbf{u} = \mathbf{d} \cdot \mathbf{v} = 0$, $\mathbf{a}^2 = \mathbf{a}_0^2$, and $\mathbf{b}^2 = \mathbf{b}_0^2$. We substitute α and β to obtain a cubic equation in $\sin\psi$ and $\cos\psi$, which yields a degree-six polynomial in $t = \tan(\psi/2)$. The contact point is $\mathbf{p} - r\mathbf{d}/\|\mathbf{d}\|$.

4.2 cylinder/sphere

Contact occurs when the distance between the cylinder axis and the sphere center equals the sum of the signed

radii, which must be positive. The distance equals the length of the line segment $\mathbf{d} = \mathbf{p} - \mathbf{q}$ that connects the cylinder axis to the sphere center and is orthogonal to the cylinder axis. We have $\mathbf{q} = \mathbf{n} + R_\psi \mathbf{q}_0$ and $\mathbf{p}$ as before. The equation $(\mathbf{p} - \mathbf{q}) \cdot \mathbf{u} = 0$ yields $\alpha = (\mathbf{n} - \mathbf{m} - \mathbf{a} + \mathbf{q}) \cdot \mathbf{u}$ with $\mathbf{u}^2 = 1$. We substitute α to obtain a quartic equation $\mathbf{d}^2 = (r + s)^2$ in $t = \tan(\psi/2)$. The contact point is $\mathbf{p} - r\mathbf{d}/\|\mathbf{d}\|$.

4.3 plane/sphere

Contact occurs when the distance from the sphere center $\mathbf{q}$ to the plane equals the sphere radius. The sphere must be convex, so the radius is positive. We use the signed distance along the outward normal of the plane, which guarantees that the sphere lies on the outside of the planar face. The plane equation is $\mathbf{a} \cdot (\mathbf{p} - \mathbf{m}) + k = 0$ with $\mathbf{p}$ a generic point on the plane, $\mathbf{a} = R_\theta \mathbf{a}_0$ the normal, and k a constant. The contact equation is $\mathbf{a} \cdot (\mathbf{q} - \mathbf{m}) + k + r = 0$ with r the sphere radius, which is quadratic in t. The contact point is $\mathbf{q} - r\mathbf{a}$.

4.4 cylinder/circle

We derive the circle contact equations in a coordinate frame that lies at the center of the circle with the z axis perpendicular to the circle plane. We compute θ as a function ψ.

Contact occurs when the circle is tangent to the ellipse in which the xy plane intersects the cylinder. The center of the ellipse, $\mathbf{o}$, is the intersection point of the cylinder axis $\mathbf{p} = \mathbf{m} + \mathbf{a} + \alpha\mathbf{u}$ with the xy plane. We compute α by setting the z component to 0 then substitute to obtain $\mathbf{o}$ as a linear function of $\mathbf{u}$. The major axis of the ellipse is parallel to the projection of the cylinder axis onto the xy plane. Its magnitude is $a = ru_z/\sqrt{u_x^2 + u_y^2}$ and its direction is $\alpha = \tan^{-1}(u_y/u_x)$ with r the signed cylinder radius. The minor axis has magnitude r and is orthogonal to the major axis.

The circle is tangent to the ellipse when its center lies on a similar ellipse whose axes are $a + s$ and $r + s$ with s the signed circle radius. The equation of this ellipse is $(KR_\alpha[(x, y) - (o_x, o_y)])^2 = 1$ with $K = (1/a + s, 1/a + r)$ a diagonal matrix and with (x, y) an arbitrary point on the ellipse. We substitute the circle center $(0, 0)$ for (x, y) to obtain the contact equation $(KR_\alpha o)^2 = 1$ of degree six. The contact point is the intersection point of the circle and the ellipse.

4.5 plane/circle

Contact occurs when the circle is tangent to the intersection line of the plane with the xy plane. The plane equation is $\mathbf{a} \cdot (\mathbf{p} - \mathbf{m}) + k = 0$ with $\mathbf{a} = R_\theta \mathbf{a}_0$ the outward normal of the plane and k a constant. We obtain the line equation by setting $p_z = 0$, which yields

$$a_x(p_x - m_x) + a_y(p_y - m_y) + k = 0.$$

The circle is tangent to the line when the signed distance from the origin to the line equals the radius s, which is positive because the circle must be convex for contact. The equation is

$$-a_x m_x - a_y m_y + k + s\sqrt{a_x^2 + a_y^2} = 0,$$

which is quartic in t, where $t = \tan\frac{\theta}{2}$. The contact point is $s\mathbf{o}/\|\mathbf{o}\|$.

4.6 sphere/circle

Contact occurs when the circle is tangent to the intersection circle of the sphere with the xy plane. The center of the intersection circle, $\mathbf{o}$, is the projection of the sphere center $\mathbf{p} = \mathbf{m} + R_\theta \mathbf{p}_0$ onto the xy plane, which we obtain by setting $p_z = 0$. The radius is $r = \text{sign}(R)\sqrt{R^2 - p_z^2}$ with R the signed radius of the sphere. The contact equation is $\|\mathbf{o}\| = r + s$ with s the signed circle radius. The sum must be positive in which case the contact equation is quartic in t. The contact point is $s\mathbf{o}/\|\mathbf{o}\|$.

5 Implementation

We have implemented a preliminary configuration space computation program in Maple with the linear algebra and 3D geometry packages. The part shapes are in constructive solid geometry representation, which is converted to boundary representation. The program derives algebraic algebraic contact equations by substituting the rotation and translation matrices of the parts. It solves them for the contact curves (symbolically when possible), and constructs the configuration space partition with the lower envelope package, using numerical routines for contact curve intersection. Contacts between symmetric features, such as the 25 teeth contacts in Figure 2, are computed only once. All the configuration spaces in this paper were computed with that program.

6 Conclusions

We have presented the first configuration space computation algorithm for spatial fixed-axes pairs and have demonstrated a preliminary implementation on three mechanical design examples. We plan to develop a complete implementation with an interface to a standard CAD

package. We are missing a reliable and efficient algorithm for solving the contact equations. All the contacts have closed-form solutions, except possibly cylinder/cylinder and cylinder/circle. These pairs have closed-form solutions when the cylinder axis is parallel to the rotation axis, which is the most common case. Numerical solutions will probably be acceptable, notably homotopy methods. When this program is completed, we will extend our simulator and tolerance analysis to spatial systems.

The next step in our research is to handle other part geometry. We can approximate the geometry with planes, cylinders, and spheres or develop new contact equations. We plan to study the tradeoffs on pairs, such as helical gears and screws, that pose unanswered mechanical design questions. Moving beyond analysis, we plan to develop design synthesis tools based on the configuration space paradigm.

Acknowledgments

Joskowicz is supported in part by a grant from the Authority for Research and Development, The Hebrew University and by a Guastalla Faculty Fellowship Israel. Sacks is supported in part by NSF grants CCR-9617600 and CCR-9505745, by a gift from Ford Motors Company, and by the Purdue Center for Computational Image Analysis and Scientific Visualization. Both are supported by a grant from the Israel Academy of Sciences.

References

[1] Edward J. Haug. *Computer-Aided Kinematics and Dynamics of Mechanical Systems*, volume I: Basic Methods. Simon and Schuster, 1989.

[2] W. Schiehlen. *Multibody systems handbook*. Springer-Verlag, 1990.

[3] Faydor L. Litvin. *Gear Geometry and Applied Theory*. Prentice Hall, New Jersey, 1994.

[4] Max Gonzales-Palacios and Jorge Angeles. *Cam Synthesis*. Kluwer Academic Publishers, Dordrecht, Boston, London, 1993.

[5] David Baraff. *Dynamic Simulation of Non-Penetrating Rigid Bodies*. PhD thesis, Cornell University, 1992.

[6] Brian Mirtich and John Canny. Impulse-based dynamic simulation. In K. Goldberg, D. Halperin, J.C. Latombe, and R. Wilson, editors, *The Algorithmic Foundations of Robotics*. A. K. Peters, Boston, MA, 1995.

[7] Ming C. Lin, Dinesh Manocha, Jon Cohen, and Stefan Gottschalk. Collision detection: Algorithms and applications. In Jean-Paul Laumond and Mark Overmars, editors, *Algorithms for Robotic Motion and Manipulation*. A. K. Peters, Boston, MA, 1997.

[8] Jean-Claude Latombe. *Robot Motion Planning*. Kluwer Academic Publishers, 1991.

[9] Elisha Sacks and Leo Joskowicz. Computational kinematic analysis of higher pairs with multiple contacts. *Journal of Mechanical Design*, 117:269–277, 1995.

[10] Elisha Sacks. Practical sliced configuration spaces for curved planar pairs. *International Journal of Robotics Research*, 1998. to appear.

[11] Elisha Sacks and Leo Joskowicz. Dynamical simulation of planar systems with changing contacts using configuration spaces. *Journal of Mechanical Design*, 120:181–187, 1998.

[12] Elisha Sacks and Leo Joskowicz. Parametric kinematic tolerance analysis of general planar systems. *Computer-Aided Design*, 30(9):707–714, 1998.

[13] Leo Joskowicz and Elisha Sacks. Computational kinematics. *Artificial Intelligence*, 51:381–416, 1991.